

## Effects of Ferric and Chromic Salts in Physicochemical, Surface and Catalytic Properties of Pure and Doped Fe<sub>2</sub>O<sub>3</sub>-Cr<sub>2</sub>O<sub>3</sub> System

G.A. El-Shobaky<sup>#</sup>, A. I. Ahmed<sup>\*</sup> and Shaymaa E. El-Shafey

Physical Chemistry Department, National Research Center, Cairo and  
Chemistry Department, Faculty of Science, Mansoura University,  
Mansoura, Egypt.

FERRIC/CHROMIC mixed oxides having the formula 0.85 Fe<sub>2</sub>O<sub>3</sub>: 0.15 Cr<sub>2</sub>O<sub>3</sub> were obtained by thermal decomposition of the mixed hydroxides prepared from mixed nitrate and sulphate solutions using NH<sub>4</sub>OH. Pure mixed hydroxides were heated at 500°C. The doped solids were prepared by treating the precipitated hydroxides with different amounts of Li<sub>2</sub>O and K<sub>2</sub>O (0.5, 0.75 and 1.5 mol %) followed by calcination at 500°C. The techniques employed were XRD, N<sub>2</sub>-adsorption and oxidation of CO by O<sub>2</sub> at 200-300°C. The results revealed that pure and doped systems consisted of nanocrystalline phases having crystallite size varying between 8-64 nm depending on the nature of ferric and chromic salts used and dopant concentration. Pure mixed solids consisted of a mixture of  $\alpha$  and  $\gamma$ -Fe<sub>2</sub>O<sub>3</sub> phase whose crystallite size decreases by increasing the dopant concentrations. K<sub>2</sub>O-doping of the investigated systems resulted in the formation of K<sub>2</sub>FeO<sub>4</sub> together with ferric oxide phases. Li<sub>2</sub>O-doping (0.5 and 0.75 mol %) led to the formation of LiFe<sub>5</sub>O<sub>8</sub> together with  $\gamma$ -Fe<sub>2</sub>O<sub>3</sub> phase. However, the heavily Li<sub>2</sub>O-doped samples consisted entirely of LiFe<sub>5</sub>O<sub>8</sub>. The S<sub>BET</sub> of pure system prepared from ferric and chromic sulphates measured higher S<sub>BET</sub> values as compared to those prepared from mixed nitrates, whereas K<sub>2</sub>O-doping decreased the S<sub>BET</sub>. On the other hand, Li<sub>2</sub>O-doping exerted a measurable increase in the S<sub>BET</sub>. The increase was however, more pronounced in case of the system prepared by using mixed sulphate solutions. The catalytic activity was higher in case of the catalysts prepared by using mixed nitrates as compared to the catalysts prepared by using mixed sulphate solutions. The doping process led to a progressive significant increase in the catalytic activity. The increase was, however, much more pronounced in case of the catalysts prepared from the mixed sulphates. The maximum increase in the k<sub>200°C</sub> value due to doping with 1.5 mol % K<sub>2</sub>O attained 30.8% and 285% for the solids prepared from mixed nitrates and mixed sulphates, respectively. These values measured 27% and 241% in case of the catalysts prepared by using mixed nitrate and mixed sulphate solutions, respectively. The doping process did not affect the mechanism of the catalyzed reaction but increased the concentrations of active sites involved in catalytic reaction without changing their energetic nature.

**Keywords:** Nanocrystalline, Fe<sub>2</sub>O<sub>3</sub>-Cr<sub>2</sub>O<sub>3</sub>, Doping and Catalytic behavior.

The catalytic oxidation of CO by O<sub>2</sub> is considered as an effective way to minimize air pollution and is being utilized in an increasing number of practical applications<sup>(1-5)</sup>. A number of catalysts have been studied in the past decades. It was found that the

---

<sup>#</sup>Corresponding author : E-mail address: elshobaky @ yahoo.com  
gamil .elshobaky @ yahoo.com

nanoparticles are much more effective as carbon monoxide catalysts than the big-sized solids. Iron-based compounds are widely used in heterogeneous catalysis either pure or in mixtures with other elements to catalyze many reactions. Volatile organic compounds (VOCs) are the main source of air pollutants, emitted from many industrial processes and transportation activities <sup>(6)</sup>. Iron oxide,  $\alpha$ -Fe<sub>2</sub>O<sub>3</sub>, has drawn enormous attention due to a wide range of applications such as red pigments <sup>(7)</sup>, catalysts <sup>(8)</sup>, gas sensor <sup>(9)</sup> and can be used as a catalyst of carbon monoxide oxidation in the presence and absence of oxygen <sup>(10)</sup>. These applications were focused on the particle size of order of nanometer. So, superfine Fe<sub>2</sub>O<sub>3</sub> nanoparticles were evaluated as a catalyst for oxidation of carbon monoxide <sup>(11)</sup>.

The catalytic activity of a large variety of catalysts can be modified by various methods. The doping of different catalytic systems can be considered as an important parameter in modifying their catalytic activities. The doping with certain foreign oxides such as Li<sub>2</sub>O, K<sub>2</sub>O or ZnO hinders the metal oxide-support interactions thus increasing the stability of catalytically active constituents <sup>(12-17)</sup>.

The present work reports the results of a study on the influence of effects of ferric and chromic salts in physicochemical, surface and catalytic properties of pure and doped Fe<sub>2</sub>O<sub>3</sub>-Cr<sub>2</sub>O<sub>3</sub> system. The techniques employed were XRD, adsorption of N<sub>2</sub> at -196°C besides catalysis of CO oxidation by O<sub>2</sub> at different temperatures between 200-300°C.

## Experimental

### Materials

Iron (III) and chromium (III) mixed hydroxides samples were prepared by using co precipitation method. This process was carried out using an aqueous solution of ferric and chromic mixed nitrate or mixed sulphate solutions at 50°C and at a pH 8 in presence of conc. NH<sub>4</sub>OH solution subjected to bubbling by a current of dry air free from CO<sub>2</sub> flowing at a rate of 20 ml/min. The salts used were of analytical grade and supplied by BDH Company and their amounts were calculated in a manner that Fe/Cr ratio was 0.85: 0.15. The molecular formula of the prepared calcined mixed solids was 0.85Fe<sub>2</sub>O<sub>3</sub>:0.15Cr<sub>2</sub>O<sub>3</sub>. The carefully washed mixed hydroxides were dried at 120°C then heated at 500 °C for 4hr.

Three Li<sub>2</sub>O-doped and three K<sub>2</sub>O-doped samples were prepared by taking calculated amounts of pure mixed hydroxides with calculated amounts of Li or K nitrates dissolved in the least amount of distilled water sufficient to make pastes. The pastes were dried at 120°C till constant weight then calcined in air 500°C for 4hr. The dopant concentrations were 0.5, 0.75 and 1.5 mol % Li<sub>2</sub>O or K<sub>2</sub>O.

Pure mixed solids were designated as Fe Cr and Fe Cr-S for the solids prepared by using mixed nitrate and mixed sulphate solutions, respectively. The solids prepared by using mixed nitrate solutions and doped with K<sub>2</sub>O and Li<sub>2</sub>O were designated as Fe Cr K<sub>1</sub>, Fe Cr K<sub>2</sub>, Fe Cr K<sub>3</sub> and Fe Cr Li<sub>1</sub>, Fe Cr Li<sub>2</sub> and Fe Cr Li<sub>3</sub>. These solids contained 0.5, 0.75 and 1.5 mol% K<sub>2</sub>O or Li<sub>2</sub>O, respectively. The solids prepared by using mixed sulphate solutions and doped with K<sub>2</sub>O or Li<sub>2</sub>O were designated as Fe Cr-S K<sub>1</sub>, Fe Cr-S K<sub>2</sub>, Fe Cr-S K<sub>3</sub> and Fe Cr-S Li<sub>1</sub>, Fe Cr-S Li<sub>2</sub> and Fe Cr-S Li<sub>3</sub> containing 0.5, 0.75 and 1.5 mol%, respectively.

*Techniques**X-ray diffraction (XRD) analysis of different mixed oxides*

X-ray powder diffractograms of various investigated solids calcined at 500°C were determined using a Bruker diffractometer (Bruker D8 advance target) the scanning rate was fixed at 8° in 2θ/min for phase identification and 0.8° in 2θ/min for line broadening profile analysis, respectively. The patterns were run with Cu Kα1 with secondly monochromator ( $\lambda = 0.1545$  nm) at 40 kV and 40 mA. The crystallite size of crystalline phases present in different solids investigated was calculated from the line broadening profile analysis of the main diffraction lines of the phases present using the Scherrer equation<sup>(18)</sup>.

$$D = \frac{K\lambda}{\beta_{1/2}\cos\theta}$$

where D is the mean crystallite diameter in Å,  $\lambda$  the wave length of X-ray beam, K the Scherrer constant (0.89),  $\beta_{1/2}$  the full-width at half-maximum (FWHM) of the main diffraction peak in radian and  $\theta$  is the diffraction angle.

*Measurements of different surface characteristics*

The different surface characteristics of various adsorbents were determined from analysis of nitrogen adsorption isotherms carried out at  $-196$  °C over various solids. These characteristics include specific surface areas ( $S_{\text{BET}}$ ), total pore volume ( $V_p$ ), mean pore radius ( $\bar{r}$ ) and pore volume distribution curves ( $\Delta v/\Delta r$ ). The  $S_{\text{BET}}$  values were determined from linear portion of the BET equation. Another series of specific surface area ( $S_t$ ) was determined from  $V_t$ -t plots constructed using suitable standard t-curves depending on the values of the BET- C constant.

The specific surface area ( $S_{\text{BET}}$ ), total pore volume ( $V_p$ ), mean pore radius ( $\bar{r}$ ) and pore volume distribution curves ( $\Delta v/\Delta r$ ) of the various adsorbents were determined from nitrogen adsorption isotherms measured at  $-196$  °C using Quantachrome NOVA Automated Gas sorbometer. The values of  $V_p$  were computed from the relation  $V_p = 15.45 \times 10^{-4} \times V_{\text{st}}$  cm<sup>3</sup>/g, where  $V_{\text{st}}$  is the volume of nitrogen adsorbed at  $P/P^\circ$  tends to unity. The values of  $\bar{r}$  were determined from the equation

$$\bar{r}(\text{Å}) = \frac{2V_p}{S_{\text{BET}}} \times 10^4 \text{ Å}$$

*Apparatus for measuring the catalytic activity*

Catalytic oxidation of CO by O<sub>2</sub> over the various catalysts was carried out at temperatures in the range of 200–300°C using a static method. A stoichiometric mixture of CO and O<sub>2</sub> (CO + 1/2 O<sub>2</sub>) at a pressure of 2 Torr was used. A fresh catalyst sample (200 mg) was employed for each kinetic experiment and was activated by heating under a reduced pressure of 10<sup>-6</sup> Torr for 1 hr at 250°C. The CO<sub>2</sub> produced was removed from the reaction system by freezing in a liquid nitrogen trap. The kinetics of the catalytic reaction was monitored by measuring the pressure of the reacting gases at different time intervals until no change in pressure was attained. The percentage decrease in pressure at a given time determines the percentage conversion

of the catalytic reaction at that time. The saturation vapour pressure of CO at  $-196^{\circ}\text{C}$  being 160 Torr makes its liquefaction at that pressure improbable under the employed conditions (2 Torr) <sup>(19)</sup>.

## Results and Discussion

### *XRD investigation of pure and variously K<sub>2</sub>O and Li<sub>2</sub>O-doped solids prepared from mixed nitrates and calcined at 500°C*

The XRD diffractograms of pure and variously doped solids calcined at  $500^{\circ}\text{C}$  were determined. The obtained diffractograms of pure solids and those doped with 0.5, 0.75 and 1.5 mol%  $\text{K}_2\text{O}$  are illustrated in Fig. 1-a. Examination of Fig 1-a shows the following: (i) Pure and variously  $\text{K}_2\text{O}$ -doped samples consisted of nanosized phases measuring crystallite size varying between 9-48 nm for ferric oxide phases. (ii) Doping the investigated system with  $\text{K}_2\text{O}$  followed by calcination at  $500^{\circ}\text{C}$  led to the formation of nanosized  $\text{K}_2\text{FeO}_4$  measuring a crystallite size that increases by increasing the dopant concentration and varies between 8 and 64 nm. (iii) Pure and doped solids consisted of a mixture of  $\alpha$  and  $\gamma$ - $\text{Fe}_2\text{O}_3$  phases together with the potassium ferrite phase. Figure 1-b shows the diffractograms of pure and variously  $\text{Li}_2\text{O}$ -doped solids calcined at  $500^{\circ}\text{C}$ . Inspection of Fig. 1-b shows the following: (i) Similarly as the case of  $\text{K}_2\text{O}$ -doped solids, the 0.5 and 0.75mol%  $\text{Li}_2\text{O}$ -doped samples consisted of a mixture of nanocrystalline  $\alpha$  and  $\gamma$ - $\text{Fe}_2\text{O}_3$  phases together with nanocrystalline  $\text{LiFe}_5\text{O}_8$  whose crystallite size increases slightly by increasing the amount of  $\text{Li}_2\text{O}$  present. (ii) The heavily  $\text{Li}_2\text{O}$ -doped samples consisted entirely of  $\text{LiFe}_5\text{O}_8$  phase. However, one can not exclude the presence of ferric oxides in a very poorly crystalline state that could not be detected by XRD investigation.

### *XRD investigation of pure and variously K<sub>2</sub>O and Li<sub>2</sub>O-doped solids prepared from mixed sulphates and calcined at 500°C*

The XRD diffractograms of pure and variously doped solids calcined at  $500^{\circ}\text{C}$  were determined. The obtained diffractograms are illustrated in Fig. 2-a. Examination of Fig 2-a shows the following: (i) Pure and variously  $\text{K}_2\text{O}$ -doped samples consisted of nanocrystalline phases measuring crystallite size varying between 15-42 nm for ferric oxide phase. (ii)  $\text{K}_2\text{O}$ -doping (0.5- 1.5mol %) conducted at  $500^{\circ}\text{C}$  led to the appearance of  $\gamma$ - $\text{Fe}_2\text{O}_3$  as a major phase. It is known that the crystallite of  $\gamma$ - $\text{Fe}_2\text{O}_3$  generally possess an imperfect cubic spinel structure, which is different from that of  $\alpha$ - $\text{Fe}_2\text{O}_3$ , hexagonal structure. The imperfect  $\gamma$ - $\text{Fe}_2\text{O}_3$  spinel allows promoter such as Cr to be incorporated into vacant sites in the  $\gamma$ - $\text{Fe}_2\text{O}_3$  resulting in less sintering of active phase in the catalysts consisting of  $\gamma$ - $\text{Fe}_2\text{O}_3$  than those consisting of  $\alpha$ - $\text{Fe}_2\text{O}_3$  employed under identical operating conditions <sup>(20)</sup>. (iii) Doping the system investigated with 0.5- 1.5 mol%  $\text{K}_2\text{O}$  followed by calcination at  $500^{\circ}\text{C}$  led to the appearance of new diffraction lines at  $d= 2.97\text{\AA}$  and  $2.94\text{\AA}$  corresponding to  $\text{K}_2\text{FeO}_4$ , JCPDS-ICDD 25-652.

Figure 2-b shows the diffractograms of pure and variously  $\text{Li}_2\text{O}$  doped solids calcined at  $500^{\circ}\text{C}$ . Inspection of Fig. 2-b shows the following: (i) Pure and variously  $\text{Li}_2\text{O}$ -doped samples consisted of nanocrystalline phases measuring crystallite size varying between 9-48 nm for ferric oxide phase. (ii) Similarly, as the case of  $\text{K}_2\text{O}$ -doped

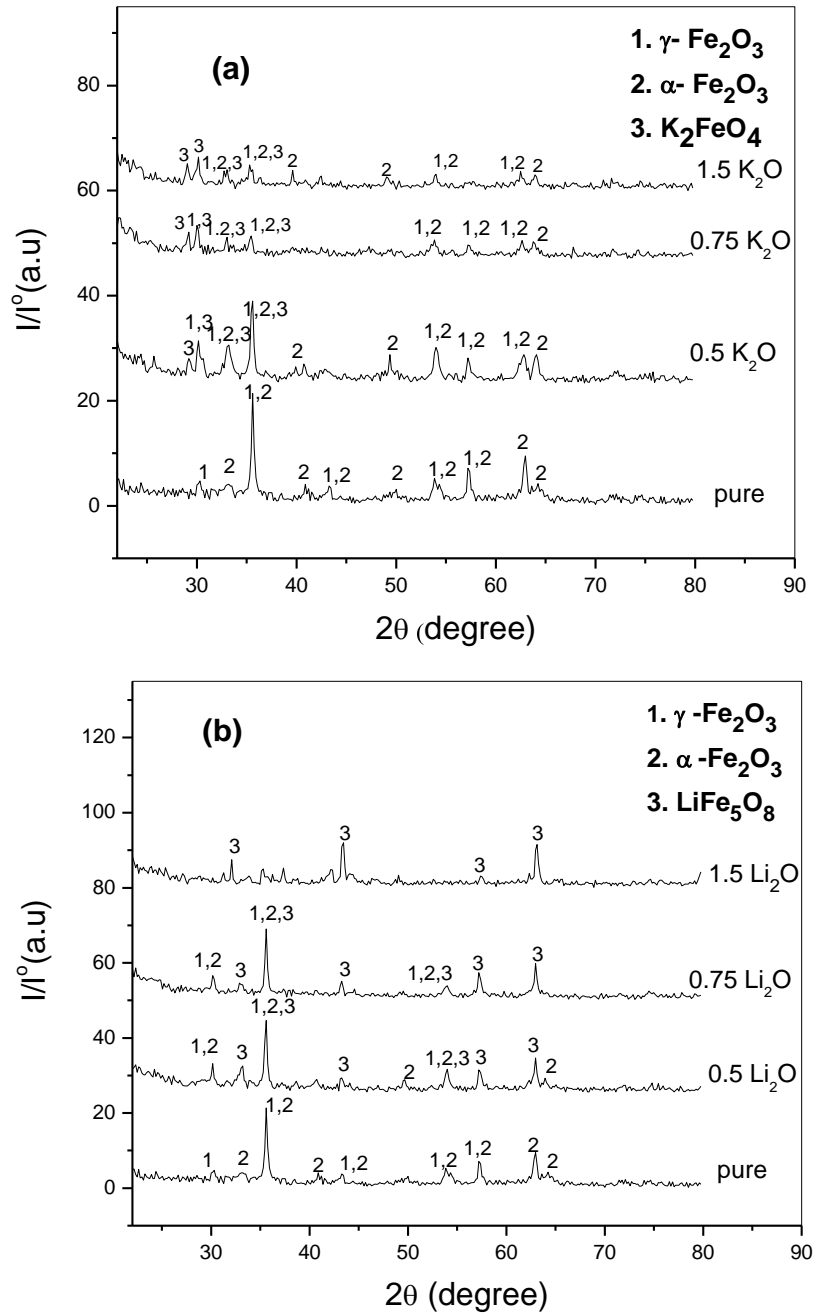


Fig. 1. X-ray diffractograms of pure and 0.5, 0.75 and 1.5 mol%: (a)  $K_2O$  and (b)  $Li_2O$ -doped samples prepared by using mixed nitrates and calcined at  $500^\circ\text{C}$ .

solids, the 0.5 and 0.75 mol%  $\text{Li}_2\text{O}$ -doped system consisted of a mixture of nanocrystalline  $\alpha$  and  $\gamma$ - $\text{Fe}_2\text{O}_3$  phases together with nanocrystalline  $\text{LiFe}_5\text{O}_8$  whose crystallite size increases slightly by increasing the amount of  $\text{Li}_2\text{O}$  present. (ii) However doping the mixed solid samples with 1.5 mole %  $\text{Li}_2\text{O}$  followed by calcination at  $500^\circ\text{C}$  led to the disappearance of both  $\alpha$ - and  $\gamma$ - $\text{Fe}_2\text{O}_3$  phases and  $\text{LiFe}_5\text{O}_8$  was the only phase present. However, one can not exclude the presence of ferric oxides in a very poorly crystalline state that could not be detected by XRD investigation.

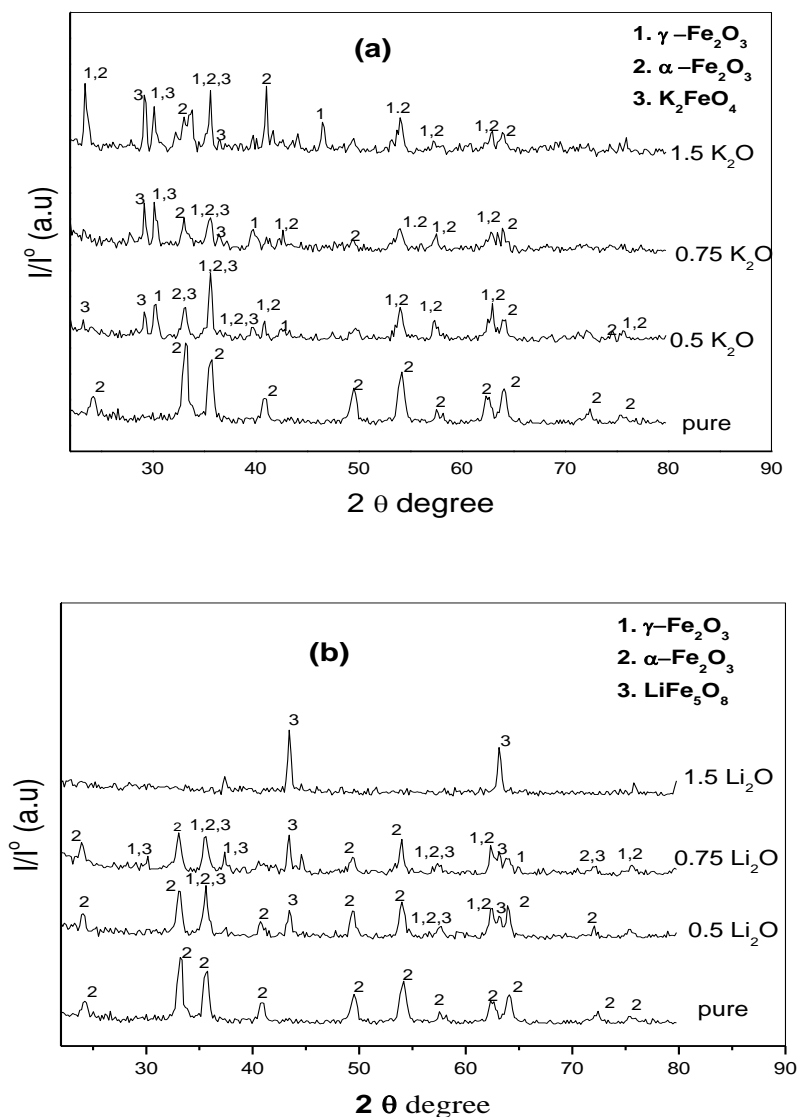


Fig. 2. X-ray diffractograms of pure and 0.5, 0.75 and 1.5 mol%: (a)  $\text{K}_2\text{O}$  and (b)  $\text{Li}_2\text{O}$ -doped samples prepared by using mixed sulphates solution and calcined at  $500^\circ\text{C}$ .

The crystallite size and degree of crystallinity of different crystalline phases in  $K_2O$  and  $Li_2O$ -doped solids calcined at  $500^\circ C$  for the solids prepared from mixed nitrates and sulphates, respectively, are given in Tables 1 & 2. It is clearly shown from these tables that  $K_2O$  and  $Li_2O$ -doping (0.5- 1.5 mol%) conducted at  $500^\circ C$  increased the degree of crystallinity and crystallite size of phases present which consisted of a mixture of alpha and gamma ferric oxides together with  $K_2FeO_4$  and  $LiFe_5O_8$  phases.

**TABLE 1. XRD data of Fe Cr, Fe Cr  $K_1$ , Fe Cr  $K_2$ , Fe Cr  $K_3$  and Fe Cr  $Li_1$ , Fe Cr  $Li_2$ , Fe Cr  $Li_3$  solids prepared by thermal decomposition at  $500^\circ C$  of their mixed hydroxides prepared from ferric and chromic mixed nitrates.**

Catalyst	Phases present	Crystallite size (nm)	Degree of crystallinity (a.u.)*
Fe Cr	$\gamma$ - $Fe_2O_3$	38	22
	$\alpha$ - $Fe_2O_3$	9	5
Fe Cr $K_1$	$\gamma$ - $Fe_2O_3$	43	18
	$\alpha$ - $Fe_2O_3$	19	9
	$K_2FeO_4$	22	8
Fe Cr $K_2$	$K_2FeO_4$	43	7
	$\alpha$ - $Fe_2O_3$	48	4
	$\gamma$ - $Fe_2O_3$	39	4
Fe Cr $K_3$	$\gamma$ - $Fe_2O_3$	40	13
	$K_2FeO_4$	64	12
	$\alpha$ - $Fe_2O_3$	15	8
Fe Cr $Li_1$	$\gamma$ - $Fe_2O_3$	39	13
	$\alpha$ - $Fe_2O_3$	31	12
	$LiFe_5O_8$	50	6
Fe Cr $Li_2$	$\gamma$ - $Fe_2O_3$	29	12
	$LiFe_5O_8$	63	11
	$\alpha$ - $Fe_2O_3$	24	10
Fe Cr $Li_3$	$LiFe_5O_8$	53	16

\* The peak area of the main diffraction lines of  $\alpha$ - and  $\gamma$ -  $Fe_2O_3$  was taken as a measure of degree of crystallinity of these phases.

Detection of potassium and lithium ferrite phases in variously doped solids in spite of the very small amounts of the dopant added (0.88 and 0.87 wt%  $Li_2O$  and  $K_2O$  in the heavily doped samples). These values are far below the detection limit of the X-ray diffractometer employed. This finding suggested clearly the enriched presence of the dopant substrate in the top surface layers of the dopant solids <sup>(21)</sup>. The enriched presence of the dopant substrate might be tentatively attributed to the fact that the doped solids were prepared by wet impregnation method and not by co-precipitation method. The disappearance of ferric oxide phases could be tentatively attributed to the solid-solid interaction between  $K_2O$  and-or  $Li_2O$  and all surface ferric oxides leading to the formation of potassium and lithium ferrite phases.

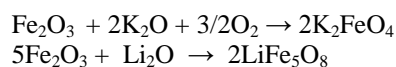


**TABLE 2. XRD data of Fe Cr, Fe Cr K<sub>1</sub>, Fe Cr K<sub>2</sub>, Fe Cr K<sub>3</sub> and Fe Cr Li<sub>1</sub>, Fe Cr Li<sub>2</sub>, Fe Cr Li<sub>3</sub> solids prepared by thermal decomposition at 500°C of their mixed hydroxides prepared from ferric and chromic mixed sulphates.**

Catalyst	Phases present	Crystallite Size (nm)	Degree of Crystallinity (a.u.)*
Fe Cr-S	$\alpha$ -Fe <sub>2</sub> O <sub>3</sub>	22	12
Fe Cr-S K <sub>1</sub>	$\gamma$ -Fe <sub>2</sub> O <sub>3</sub>	37	16
	K <sub>2</sub> FeO <sub>4</sub>	34	8
	$\alpha$ -Fe <sub>2</sub> O <sub>3</sub>	25	7
Fe Cr-S K <sub>2</sub>	K <sub>2</sub> FeO <sub>4</sub>	69	11
	$\gamma$ -Fe <sub>2</sub> O <sub>3</sub>	39	7
	$\alpha$ -Fe <sub>2</sub> O <sub>3</sub>	42	8
Fe Cr-S K <sub>3</sub>	$\gamma$ -Fe <sub>2</sub> O <sub>3</sub>	40	13
	K <sub>2</sub> FeO <sub>4</sub>	64	12
	$\alpha$ -Fe <sub>2</sub> O <sub>3</sub>	15	8
Fe Cr-S Li <sub>1</sub>	$\gamma$ -Fe <sub>2</sub> O <sub>3</sub>	39	13
	$\alpha$ -Fe <sub>2</sub> O <sub>3</sub>	31	12
	LiFe <sub>5</sub> O <sub>8</sub>	50	6
Fe Cr-S Li <sub>2</sub>	$\gamma$ -Fe <sub>2</sub> O <sub>3</sub>	29	12
	LiFe <sub>5</sub> O <sub>8</sub>	63	11
	$\alpha$ -Fe <sub>2</sub> O <sub>3</sub>	24	10
Fe Cr-S Li <sub>3</sub>	LiFe <sub>5</sub> O <sub>8</sub>	53	16

\*The peak area of the main diffraction lines of  $\alpha$ - and  $\gamma$ -Fe<sub>2</sub>O<sub>3</sub> was taken as a measure of degree of crystallinity of these phases.

*Surface properties of pure and doped solids prepared from ferric and chromic mixed nitrates*

The different surface characteristics of pure and variously doped adsorbents were determined by analysis of N<sub>2</sub> adsorption isotherms measured at -196°C over various adsorbents. These isotherms, not given, belong to type II of BDDT classification. These characteristics include specific surface area ( $S_{\text{BET}}$ ), total pore volume ( $V_p$ ), mean pore radius ( $r^-$ ) and pore volume distribution curves ( $\Delta v/\Delta r$ ). The  $S_{\text{BET}}$  values were determined from linear portion of the BET equation. Another series of specific surface area ( $S_t$ ) was determined from  $V_t$  plots constructed using suitable standard t-curves of de Boer<sup>(22)</sup>.

The results obtained are given in Table 3. Examination of Table 3 shows the following: (i) The values of  $S_{\text{BET}}$  and  $S_t$  of all adsorbents investigated are close to each other which justifies the correct choice of standard t-curve used in pore analysis and indicates the absence of the ultra micro pores. (ii) Doping the system investigated with the smallest amount of K<sub>2</sub>O led to a measurable decrease in the  $S_{\text{BET}}$  values which remained almost unchanged by increasing the dopant concentration. (ii) K<sub>2</sub>O-doping resulted in a progressive significant decrease in  $r^-$  (an effective progressive pore narrowing) which decreased from 83 to 20 Å in presence of 1.5 mol% K<sub>2</sub>O. This decrease might be expected to increase the  $S_{\text{BET}}$ . This expectation has not been verified experimentally. So, the observed decrease in  $S_{\text{BET}}$  due to doping with K<sub>2</sub>O might be

tentatively attributed to the considerable drop in the  $V_p$  value due to this process. In fact,  $V_p$  decreases from 0.217 to 0.036 up on doping with 1.5 mol%  $K_2O$ .

**TABLE 3. Surface characteristics of pure and variously  $K_2O$  and  $Li_2O$ -doped  $Fe_2O_3$ - $Cr_2O_3$  solids prepared by thermal decomposition at  $500^\circ C$  of their mixed hydroxides prepared from ferric and chromic mixed nitrates.**

Adsorbent	$S_{BET}$ $m^2/g$	$S_t$ $m^2/g$	Total pore volume $V_p$ , cc/g	Mean pore radius $r$ Å	BET-C constant
Fe Cr	52	54	0.21658	83	152
Fe Cr $K_1$	37	35	0.0555	30	3
Fe Cr $K_2$	35	32	0.03697	21	3
Fe Cr $K_3$	37	33	0.03635	20	3
Fe Cr $Li_1$	61	58	0.1106	36	5
Fe Cr $Li_2$	103	99	0.16243	32	4
Fe Cr $Li_3$	7.4	7.2	0.0242	65	-9

Examination of surface characteristics of  $Li_2O$ -doped solids (*c.f.* Table 3) shows the following: (i) The values of  $S_{BET}$  and  $S_t$  for all adsorbents investigated are close to each other which justifies the correct choice of standard t-curve used in pore analysis and indicates the absence of the ultra micro pores. (ii) Opposite to  $K_2O$ -doping  $Li_2O$ -doping of the system investigated (0.5 and 0.75 mol%  $Li_2O$ ) resulted in a measurable significant increase in the  $S_{BET}$ ; the increase attained 98% for the sample doped with 0.75 mol%  $Li_2O$ . (iii) The increase in the dopant concentration up to 1.5 mol% led to a sudden drop in the  $S_{BET}$ . This significant decrease in the  $S_{BET}$  value in the heavily  $Li_2O$  doped sample could be discussed in terms of the considerable drop in the numbers of pores present. In fact, the  $V_p$  value decreases from 0.217 to 0.024cc/g. This dropping in the  $S_{BET}$  could be also attributed to the complete conversion of ferric oxide phases into  $LiFe_5O_8$  phase.

The pore volume distribution curves ( $\Delta v/\Delta r$ ) for pure and heavily doped adsorbents calcined at  $500^\circ C$  were determined. The curves obtained are illustrated in Fig 3. These curves show multimodal distribution for pores present in pure and  $Li_2O$ -doped adsorbents. The maxima of the most probable pore radius are located at 18, 29 and  $46\text{Å}$  for pure solid calcined at  $500^\circ C$  and at 15, 18 and  $54\text{Å}$  for 1.5 mol%-doped solid calcined at the same temperature. However, the majority of pores present in the doped adsorbent measured pore radius between 15 and  $18\text{Å}$ . On the other hand, ( $\Delta v/\Delta r$ ) curve of adsorbent doped with 1.5 mol%  $K_2O$  shows unimodal distribution of pores present at a value of  $36\text{Å}$ . These findings might suggest that  $K_2O$ -doping led to the widening

of pores present. K<sub>2</sub>O-doping shifted the value of most probable pore radius from 18, 29 Å to 36 Å. The comparison between the areas of ( $\Delta v/\Delta r$ ) curves shows that the doping process conducted at 500°C decreased the volume of pores present. The decrease was, however, more pronounced in case of Li<sub>2</sub>O-doping. These results agree well with the V<sub>p</sub> values measured for pure and doped solids calcined at 500°C (*c.f.* Table 3).

*Surface properties of pure and doped solids prepared from ferric and chromic mixed sulphates*

The results obtained are given in Table 4. Examination of Table 4 shows the following: (i) The values of S<sub>BET</sub> and S<sub>t</sub> for all adsorbents investigated are close to each other which justifies the correct choice of standard t-curve used in pore analysis and indicates the absence of the ultra micro pores. (ii) Doping the system investigated with the smallest amount of K<sub>2</sub>O led to a progressive measurable decrease in the S<sub>BET</sub> values. This decrease reaches to about 29% , 39% and 48% for 0.5 , 0.75 and 1.5 mol% K<sub>2</sub>O-doped samples, respectively (iii) K<sub>2</sub>O doping resulted in a progressive significant decrease in  $r^-$  (an effective progressive pore narrowing) which decreased from 44 to 19 Å in presence of 1.5 mol% K<sub>2</sub>O. This decrease might be expected to increase the S<sub>BET</sub>. This expectation has not been verified experimentally. So, the observed decrease in S<sub>BET</sub> due to doping with K<sub>2</sub>O might be tentatively attributed to the considerable drop in the V<sub>p</sub> value due to this process. In fact, V<sub>p</sub> decreased from 0.193 to 0.043 cc/g upon doping with 1.5 mol% K<sub>2</sub>O. The decrease in S<sub>BET</sub> values might be also attributed to a possible location of some of K<sub>2</sub>O in the pores of the system investigated leading to their blocking. Furthermore, the decrease in specific surface area might be also attributed to the formation of potassium ferrite. The formation of this compound might be accompanied by a significant loss in their porosity followed by a corresponding decrease in their S<sub>BET</sub> values.

The surface characteristics of variously Li<sub>2</sub>O-doped adsorbents subjected to heating at 500°C were determined. Examination of surface characteristics of Li<sub>2</sub>O-doped solids (*c.f.* Table.4) shows the following:: (i) The values of S<sub>BET</sub> and S<sub>t</sub> for all adsorbents investigated are close to each other which justifies the correct choice of standard t-curve used in pore analysis and indicates the absence of the ultra micro pores. (ii) Treatment of the investigated system with 0.5 mol% of Li<sub>2</sub>O followed by calcination at 500°C led to an increase in its S<sub>BET</sub> of about 26%. The observed increase in the S<sub>BET</sub> of Fe<sub>2</sub>O<sub>3</sub>/Cr<sub>2</sub>O<sub>3</sub> system due to doping with the smallest amount of Li<sub>2</sub>O (0.5 mol%) could be attributed to the creation of new pores during the thermal treatment of the doped solids via liberation nitrogen oxides gases during thermal decomposition of LiNO<sub>3</sub> dopant added. Similar results have been reported in the case of CuO/Al<sub>2</sub>O<sub>3</sub> <sup>(23)</sup>, CuO-ZnO/Al<sub>2</sub>O<sub>3</sub> <sup>(24)</sup> Cr<sub>2</sub>O<sub>3</sub>/Al<sub>2</sub>O<sub>3</sub> <sup>(25)</sup> and NiO/Al<sub>2</sub>O<sub>3</sub> systems <sup>(26)</sup>. (iii) On the other hand, Li<sub>2</sub>O-doping decreased the S<sub>BET</sub> to an extent proportional to the amount of dopant added. The decrease attained 22% for the heavily doped samples. This significant decrease in the S<sub>BET</sub> value in the heavily Li<sub>2</sub>O doped sample could be discussed in terms of the considerable drop in the numbers of pores present. In fact, the V<sub>p</sub> value decreases from 0.194 to 0.084 cc/g and could be also attributed to the complete conversion of ferric oxide phases into LiFe<sub>5</sub>O<sub>8</sub> phase.

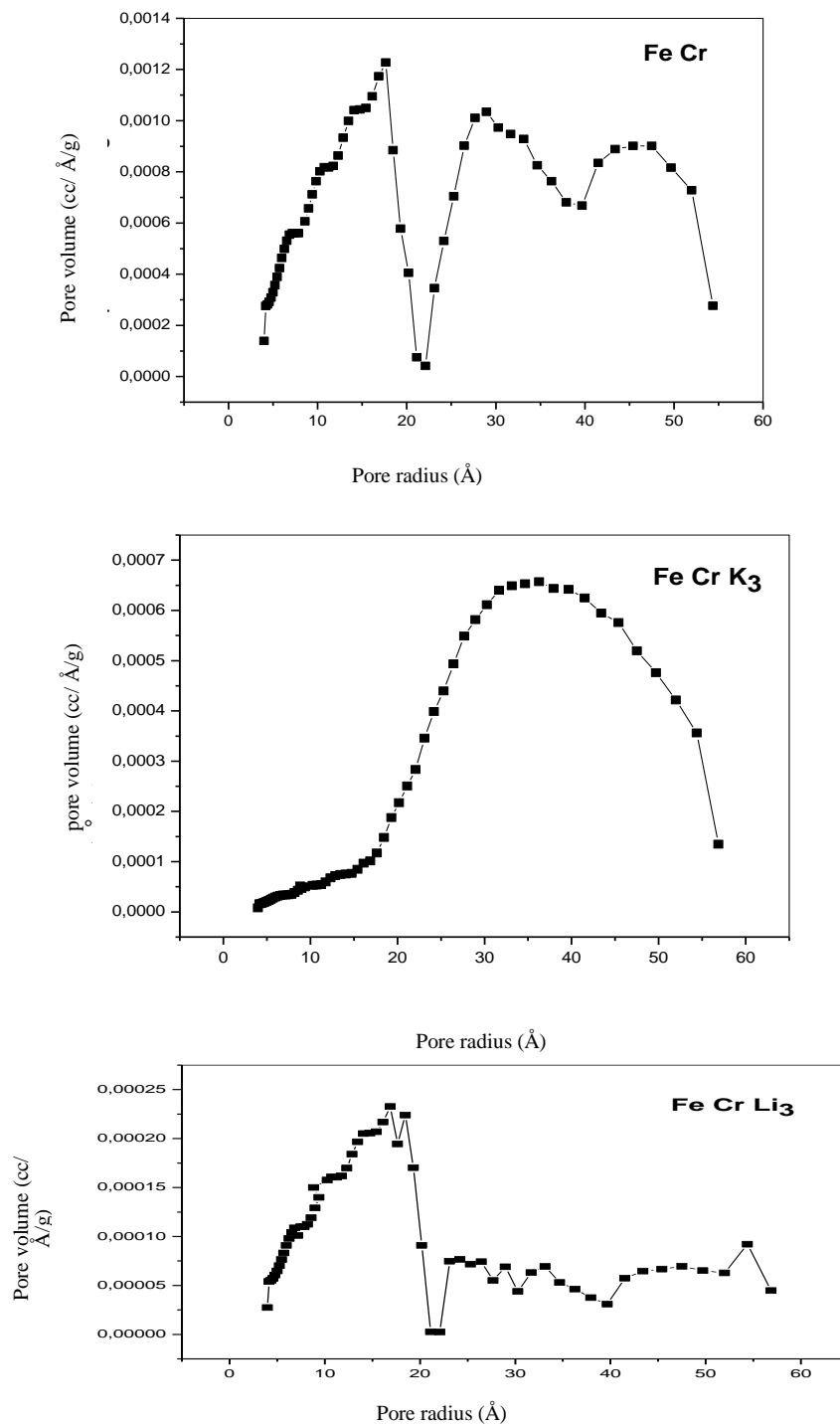


Fig. 3. Pore volume distribution curves of Fe Cr, Fe Cr K<sub>3</sub> and Fe Cr Li<sub>3</sub> samples calcined at 500°C.

**TABLE 4.** Surface characteristics of pure and K<sub>2</sub>O-or Li<sub>2</sub>O-doped Fe<sub>2</sub>O<sub>3</sub>- Cr<sub>2</sub>O<sub>3</sub> solids prepared using thermal decomposition of their mixed hydroxides at 500°C using ferric and chromic mixed sulphates

Adsorbent	S <sub>BET</sub> m <sup>2</sup> /g	S <sub>t</sub> m <sup>2</sup> /g	Total pore volume V <sub>p</sub> , cc/g	Mean pore radius r̄, Å	BET-C constant
Fe Cr	87	85	0.19352	44	1
Fe Cr-S K <sub>1</sub>	62	60	0.07967	26	3
Fe Cr-S K <sub>2</sub>	53	52	0.0881	33	2
Fe Cr-S K <sub>3</sub>	45	46	0.0433	19	2
Fe Cr-S Li <sub>1</sub>	110	112	0.25307	46	4
Fe Cr-S Li <sub>2</sub>	78	77	0.1067	27	3
Fe Cr-S Li <sub>3</sub>	68	70	0.0835	25	3

**TABLE 5.** Reaction rate constant per unit mass ( $k \times 10^{-3} \text{ min}^{-1} \text{ g}^{-1}$ ) for the catalytic reaction carried out at 200-300°C over pure and Li<sub>2</sub>O or K<sub>2</sub>O-doped Fe<sub>2</sub>O<sub>3</sub>-Cr<sub>2</sub>O<sub>3</sub> solids calcined at 500°C and prepared using ferric and chromic mixed nitrates.

Catalyst	Reaction temperature °C	$k \times 10^{-3}$ $\text{min}^{-1} \text{ g}^{-1}$
Fe Cr	200	7.8
	250	8.1
	300	8.9
Fe Cr K <sub>1</sub>	200	9
	250	10
	300	11
Fe Cr K <sub>2</sub>	200	9.6
	250	11.1
	300	11.2
Fe Cr K <sub>3</sub>	200	10.2
	250	10.8
	300	11.5
Fe Cr Li <sub>1</sub>	200	8.8
	250	9.3
	300	10.1
Fe Cr Li <sub>2</sub>	200	9.1
	250	9.7
	300	10.9
Fe Cr Li <sub>3</sub>	200	9.9
	250	10.1
	300	10.4

The pore volume distribution curves ( $\Delta v/\Delta r$ ) for pure and heavily doped adsorbents calcined at 500°C were determined. The curves obtained are illustrated in Fig 4. These curves show multimodal distribution for pores present in pure and adsorbent. The maxima of the most probable pore radius are located at 18, 28 and 40 Å for pure solid calcined at 500°C. On the other hand, ( $\Delta v/\Delta r$ ) curve of adsorbent doped with 1.5 mol% K<sub>2</sub>O and 1.5 mol% Li<sub>2</sub>O shows unimodal distribution of pores present at a value of 36 Å. These findings might suggest that K<sub>2</sub>O and Li<sub>2</sub>O-doping led to the widening of pores present. K<sub>2</sub>O and Li<sub>2</sub>O-doping shifted the value of most probable pore radius from 18, 28 Å to 36 Å. The comparison between the areas of ( $\Delta v/\Delta r$ ) curves shows that the doping process conducted at 500°C decreased the volume of pores present. The decrease was, however, more pronounced in case of K<sub>2</sub>O-doping. These results agree well with the V<sub>p</sub> values measured for pure and doped solids calcined at 500°C (*c.f.* Table 3).

*Catalytic activity of pure and variously doped solids prepared from mixed nitrates*

The oxidation of CO by O<sub>2</sub> at 200-300°C was carried out over pure and variously doped solids calcined at 500°C. First order kinetics was observed in all cases; the slopes of the first order plots determine the values of reaction rate constant ( $k$ ) measured at a given temperature over a given catalyst sample. Figure 5 shows representative first order-plots of CO oxidation by O<sub>2</sub> carried out at 200, 250, and 300°C over Fe Cr, Fe Cr K<sub>3</sub> and Fe Cr Li<sub>3</sub> samples calcined at 500°C. The computed  $k$  values are given in Table 5. Examination of Table 5 shows the following:  $k$  increases progressively upon increasing the amounts of Li<sub>2</sub>O or K<sub>2</sub>O added in the doped solids. The maximum increase in the  $k$  value due to doping with 1.5 mol% Li<sub>2</sub>O or 1.5 mol% K<sub>2</sub>O for the reaction carried out at 200°C attained 26.9% and 30.8%, respectively. These results clearly indicate the role of the nature of dopant in modifying the catalytic activity in CO oxidation by O<sub>2</sub>.

The parameters which determine the catalytic activity of Fe<sub>2</sub>O<sub>3</sub>/Cr<sub>2</sub>O<sub>3</sub> system include the concentration of catalytically active constituents on the top surface layers of treated solids and their possible interactions. The doping process might affect the number of active sites on the catalyst's surface contributing in chemisorption and catalysis of CO-oxidation by O<sub>2</sub>. The energetic nature of these sites could be also influenced by doping. Furthermore, the mechanism of the catalytic reaction could be altered by doping.

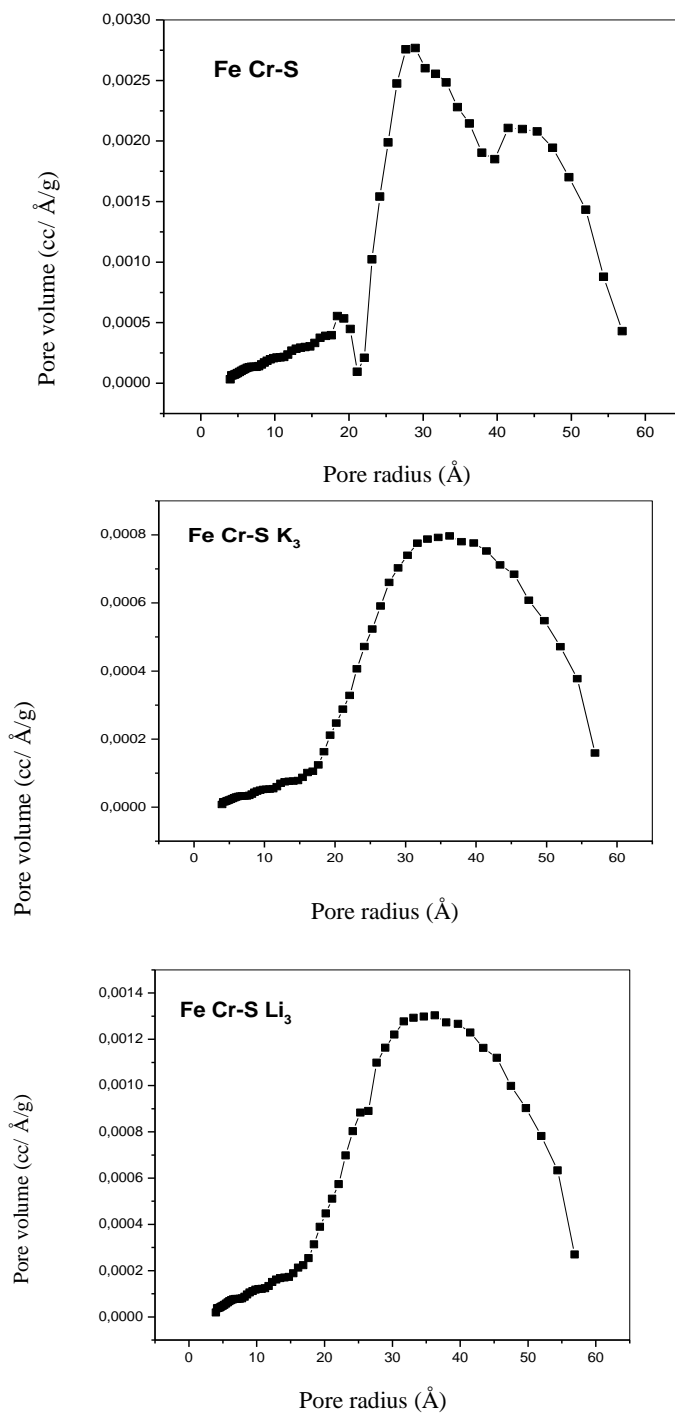


**Fig. 4.** Pore volume distribution curves of Fe Cr-S, Fe Cr-S K<sub>3</sub> and Fe Cr-S Li<sub>3</sub> samples calcined at 500°C.

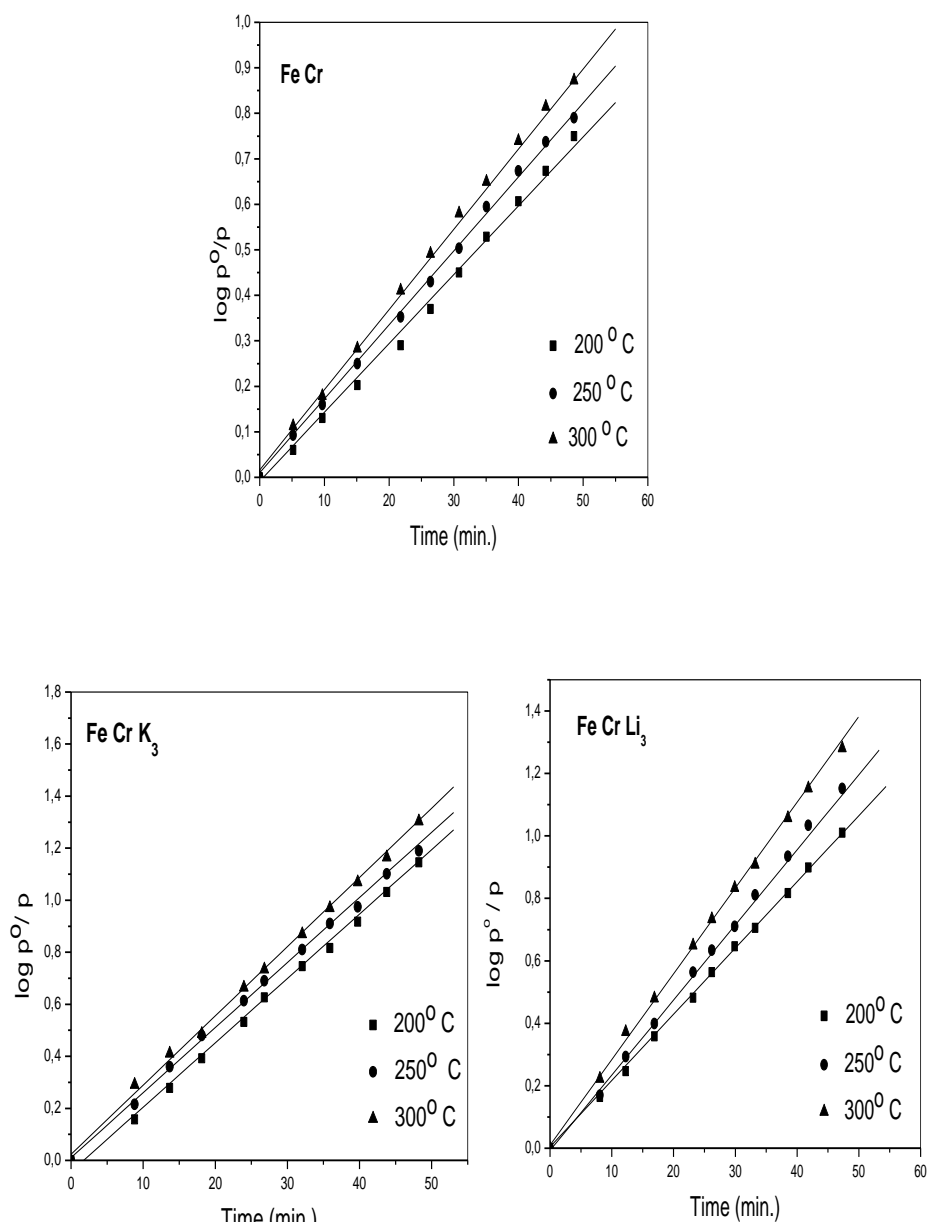


Fig. 5. First order-plots of CO oxidation by O<sub>2</sub> carried out at different temperatures over Fe Cr, Fe Cr K<sub>3</sub> and Fe Cr Li<sub>3</sub> systems calcined at 500°C.

The change in the catalytic activity of the system investigated due to doping either with  $K_2O$  or  $Li_2O$  could be discussed in terms of the following parameters: (i) The change in  $S_{BET}$ , (ii) The change in the crystallite size of the catalytically active constituents (some of surface  $Fe_2O_3$ ), (iii) Conversion of some of  $\alpha$ - $Fe_2O_3$  into  $\gamma$ - $Fe_2O_3$ , (iv) Conversion of some of  $Fe_2O_3$  into lithium or potassium ferrites. The increase in the  $S_{BET}$  is normally accompanied by an increase in the activity. The decrease in the crystallite size of  $Fe_2O_3$  might be also followed by an increase in the catalytic activity and vice versa. The formation of lithium or potassium ferrites (devoted with smaller activity compared to  $Fe_2O_3$ ) might decrease the catalytic activity of the doped solids. In order to account for the induced change in the  $S_{BET}$ , the reaction rate constant per unit surface area ( $k^-$ ) was calculated and the computed values for the reaction carried out at  $200^\circ C$  were  $15 \times 10^{-5}$ ,  $24.3 \times 10^{-5}$ ,  $27.4 \times 10^{-5}$  and  $27.6 \times 10^{-5} \text{ min}^{-1} \text{ m}^{-2}$  for pure sample and those doped with 0.5, 0.75 and 1.5 mol%  $K_2O$ , respectively. The maximum increase in the  $k^-_{200^\circ C}$  value due to doping with 1.5 mol%  $K_2O$  reached 84%. The  $k^-_{200^\circ C}$  values for the variously  $Li_2O$ -doped samples are  $14.4 \times 10^{-5}$ ,  $8.8 \times 10^{-5}$  and  $133.8 \times 10^{-5} \text{ min}^{-1} \text{ m}^{-2}$  for 0.5, 0.75 and 1.5  $Li_2O$ -doped solids, respectively. So, the maximum increase in the  $k^-_{200^\circ C}$  due to doping with 1.5 mol %  $Li_2O$  reached a considerable value (892%). This value might be attributed to an effective sintering of the heavily doped catalyst (the  $S_{BET}$  decreased from 52 to  $4.7 \text{ m}^2/\text{g}$ ).

The fact that the computed  $k^-$  values for the catalytic reaction carried out at  $200^\circ C$  are different from each other and indicated that the doping process increased the catalytic activity of the investigated system. The increase was, however, more pronounced in case of  $K_2O$ -doping. Furthermore, the induced changes in the specific surface area due to doping are not a dominant parameter determining the catalytic activity of the system investigated. The formation of lithium and potassium ferrites in the doped solids might decrease their catalytic activity. This expectation was not verified experimentally since an increase and not decrease in the activity was found. So, one might expect that the doping process might increase the portion of  $Fe_2O_3$  phases involved directly in the catalytic reaction.

#### *Effects of $Li_2O$ and $K_2O$ -doping on $\Delta E$ of the catalyzed reaction prepared from mixed nitrates*

Determination of the apparent activation energy ( $\Delta E$ ) for the catalysis of CO oxidation by  $O_2$  over pure and variously doped solids precalcined at  $500^\circ C$  may shed some light on the possible change in the mechanism of the catalyzed reaction and hence gives useful information about the possible alteration in the concentration and nature of catalytically active constituents.

The values of  $k$  measured at temperatures varying between 200 and  $300^\circ C$  over the variously doped solids enable  $\Delta E$  to be calculated by direct application of the Arrhenius equation. The calculated values of  $\Delta E$  are listed in Table 6 which also includes the values of the pre-exponential factor  $A$  of the Arrhenius equation. Table 6 shows that  $A$  changes with doping, which may be an indication of the heterogeneity of the catalyst's surface. It can be seen from the results in Table 6 that, fluctuation in  $\Delta E$  and  $\ln A$  values for the investigated solids were observed (*i.e.* both increase and decrease in their values).

**TABLE 6** Computed activation energies ( $\Delta E$ ,  $\Delta E^*$ ) and logarithm of pre-exponential factor of the Arrhenius equation for the catalytic reaction carried out at 200-300°C over pure and Li<sub>2</sub>O or K<sub>2</sub>O-doped Fe<sub>2</sub>O<sub>3</sub>/Cr<sub>2</sub>O<sub>3</sub> solids calcined at 500°C and prepared using ferric and chromic mixed nitrates.

Catalyst	$\Delta E$ (kJ/mol)	ln A	$\Delta E_1^*$ (kJ/mol)
Fe Cr	2.7	-1.88	2.7
Fe Cr K <sub>1</sub>	3.34	-1.54	2.8
Fe Cr K <sub>2</sub>	3.7	-1.43	2.9
Fe Cr K <sub>3</sub>	2.7	-1.58	2.9
Fe Cr Li <sub>1</sub>	3.0	-1.67	3.0
Fe Cr Li <sub>2</sub>	4.0	-1.38	2.7
Fe Cr Li <sub>3</sub>	1.0	-2.04	2.7

The fact that  $\Delta E$  and ln A values for all solids investigated fluctuate in almost the same manner might suggest that the observed changes in  $\Delta E$  values might come from corresponding change in ln A values. This speculation could be confirmed from recalculation of  $\Delta E$  values for the reaction conducted over pure and variously doped solids calcined at 500°C adopting the ln A value for pure sample to all doped solids calcined at the same temperature (500°C). The recalculated values of the activation energies ( $\Delta E^*$ ) are given in the last column of Table 6. It is clearly shown from the data given that  $\Delta E^*$  values of pure and doped solids showed almost the same values ( $2.85 \pm 0.15 \text{ kJmol}^{-1}$ ) for the solids doped with K<sub>2</sub>O and Li<sub>2</sub>O. This finding suggested clearly that doping Fe<sub>2</sub>O<sub>3</sub>/Cr<sub>2</sub>O<sub>3</sub> system either with Li<sub>2</sub>O or K<sub>2</sub>O followed by heating at 500°C did not much modify the activation energy of CO oxidation by O<sub>2</sub> over different solids but changed the concentration of active sites involved in the catalyzed reaction. This conclusion leads to an additional evidence from the plot of the equation:  $A = a \exp h \Delta E$ , derived on the basis of the dissipation function of active sites by their energy as a consequence of surface heterogeneity<sup>(27)</sup>.  $F(E_i) = a \exp h E_i$  where  $E_i$  is the energy of interaction of site 'i' with the substrate<sup>(27)</sup>. The constants "h" and "a", indicate that the doping process followed by precalcination at 500°C did not change the energetic nature of the active sites but changed their concentration on the top surface layers of the treated catalysts.

*Catalytic activity of pure and doped solids prepared by using mixed sulphate solutions*

Figure 6 shows representative first order-plots of CO oxidation by O<sub>2</sub> carried out at 200, 250, and 300°C over Fe Cr-S, Fe Cr-S K<sub>3</sub> and Fe Cr-S Li<sub>3</sub> samples calcined at 500°C. The computed *k* values were calculated for different solids measured at 200, 250 and 300°C are given in Table 7. Examination of Table 7 shows the following: *k* increases progressively upon increasing the Li<sub>2</sub>O or K<sub>2</sub>O contents in the doped solids. The increase was, however, more pronounced in case of K<sub>2</sub>O-doping. In fact, the maximum increase in the *k* value due to doping with 1.5 mol% K<sub>2</sub>O or 1.5 mol% Li<sub>2</sub>O for the reaction carried out at 200°C attained 285% and 241%, respectively. These results clearly indicate the role of the nature of dopant in modifying the catalytic activity in CO oxidation by O<sub>2</sub>.

**TABLE 7. Reaction rate constant per unit mass ( $k \times 10^{-3} \text{ min}^{-1} \text{ g}^{-1}$ ) for the catalytic reaction carried out at 200-300°C over pure and Li<sub>2</sub>O or K<sub>2</sub>O-doped Fe<sub>2</sub>O<sub>3</sub>-Cr<sub>2</sub>O<sub>3</sub> solids calcined at 500°C and prepared using ferric and chromic mixed sulphates.**

Catalyst	Reaction temperature oC	$k \times 10^{-3}$ $\text{min}^{-1} \text{g}^{-1}$
Fe Cr-S	200	3.4
	250	6.5
	300	7.5
Fe Cr-S K <sub>1</sub>	200	11
	250	12
	300	12.9
Fe Cr-S K <sub>2</sub>	200	12.2
	250	13
	300	13.9
Fe Cr-S K <sub>3</sub>	200	13.1
	250	14.3
	300	15.1
Fe Cr-S Li <sub>1</sub>	200	10.4
	250	11.2
	300	12.4
Fe Cr-S Li <sub>2</sub>	200	10.6
	250	11
	300	12.4
Fe Cr-S Li <sub>3</sub>	200	11.6
	250	13
	300	14.4

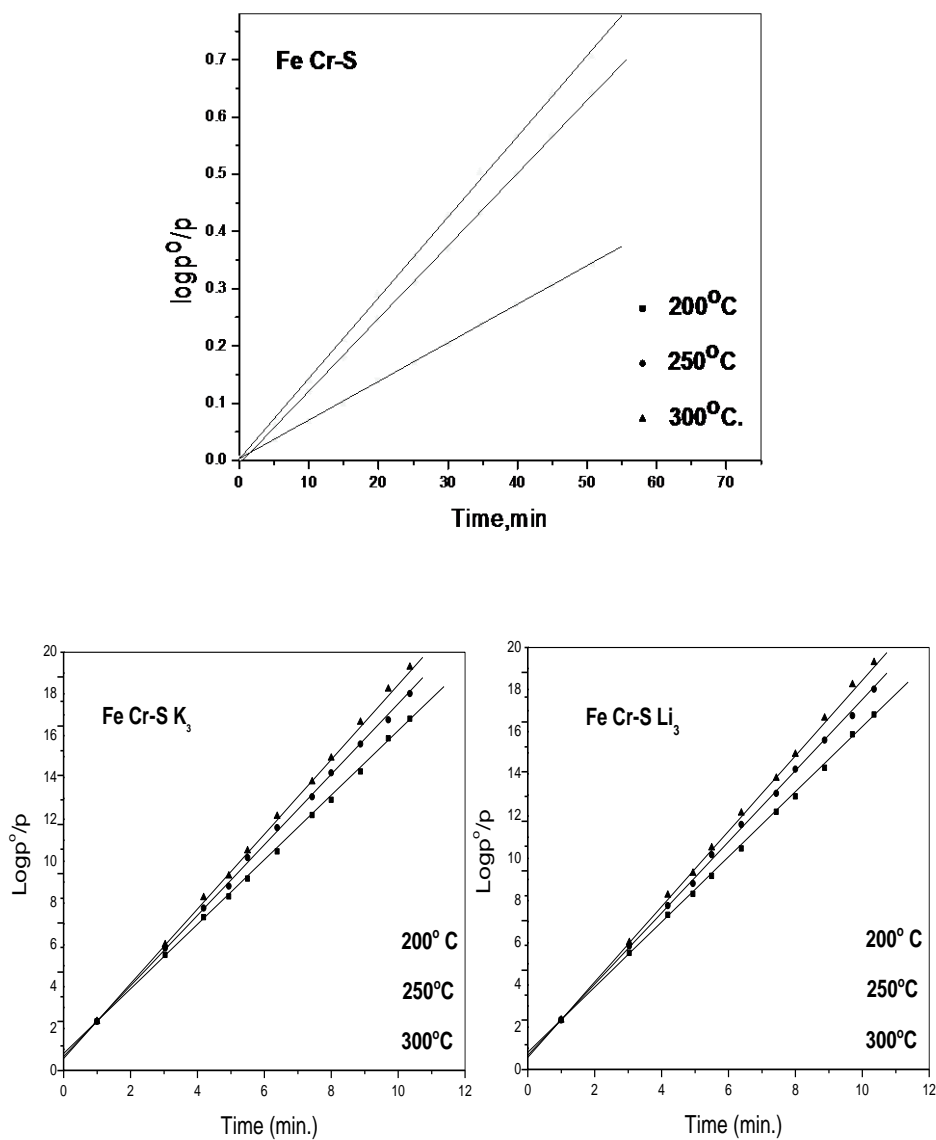


**Fig. 6.** First order-plots of CO oxidation by  $O_2$  carried out at different temperatures over Fe Cr-S, Fe Cr-S  $K_3$  and Fe Cr-S  $Li_3$  systems calcined at  $500^\circ C$ .

The change in the catalytic activity of the system investigated due to doping either with  $K_2O$  or  $Li_2O$  could be discussed in terms of the parameters previously given in the preceding section of the present work. The observed increase due to the doping process could not be attributed to induce changes in the  $S_{BET}$  of the doped solids. So, the conversion of some of  $\alpha\text{-Fe}_2O_3$  into  $\gamma\text{-Fe}_2O_3$ , devoted with higher catalytic activity, might account for the observed increase in the catalytic activity of doped solids. It is

well known that  $\gamma$ -Fe<sub>2</sub>O<sub>3</sub> is more active than  $\alpha$ -Fe<sub>2</sub>O<sub>3</sub><sup>(28)</sup>. So, the formation of  $\gamma$ -Fe<sub>2</sub>O<sub>3</sub> in the doped solids overcomes the possible decrease in the activity due to the formation of potassium and lithium ferrites.

*Effects of Li<sub>2</sub>O and K<sub>2</sub>O doping on  $\Delta E$  of the catalyzed reaction prepared from mixed sulphates*

The values of ( $\Delta E$ ) and recalculated values of the activation energies ( $\Delta E^*$ ) are given in Table 8. It is clearly shown from the data given in Table 8 that  $\Delta E^*$  values of pure and doped solids showed almost the same values ( $17 \pm 2$  kJmol<sup>-1</sup>) for solids doped with K<sub>2</sub>O and ( $18 \pm 2$  kJmol<sup>-1</sup>) for the solids doped with Li<sub>2</sub>O. This finding suggested clearly that doping Fe<sub>2</sub>O<sub>3</sub>/Cr<sub>2</sub>O<sub>3</sub> system either with Li<sub>2</sub>O or K<sub>2</sub>O followed by heating at 500°C did not much modify the activation energy of CO oxidation by O<sub>2</sub> over different solids but changed the concentration of active sites involved in the catalyzed reaction.

**TABLE 8. Computed activation energies ( $\Delta E$ ,  $\Delta E^*$ ) and logarithm of pre-exponential factor of the Arrhenius equation for the catalytic reaction carried out at 200-300°C over pure and Li<sub>2</sub>O or K<sub>2</sub>O-doped Fe<sub>2</sub>O<sub>3</sub>/Cr<sub>2</sub>O<sub>3</sub> solids calcined at 500°C and prepared using ferric and chromic mixed sulphates.**

Catalyst	$\Delta E$ (kJ/mol)	ln A	$\Delta E_1^*$ (kJ/mol)
Fe Cr-S	19.2	1.68	19.2
Fe Cr-S K <sub>1</sub>	3.6	-1.28	16.5
Fe Cr-S K <sub>2</sub>	3.3	-1.28	16.2
Fe Cr-S K <sub>3</sub>	7.9	-0.125	15.7
Fe Cr-S Li <sub>1</sub>	4.1	-1.25	16.8
Fe Cr-S Li <sub>2</sub>	3.7	-1.35	16.9
Fe Cr-S Li <sub>3</sub>	2.6	-1.44	16.2

### Conclusions

The results obtained permitted to draw the following main conclusions: Physicochemical, surface and catalytic properties of pure and variously K<sub>2</sub>O and Li<sub>2</sub>O-doped Fe<sub>2</sub>O<sub>3</sub>/Cr<sub>2</sub>O<sub>3</sub> solids were much influenced by the nature of ferric and chromic salts used in the preparation of the mixed hydroxides. However, all prepared solids consisted of nanocrystalline phases having crystallite size between 8-64 nm.

- Pure mixed solids calcined at 500°C and prepared by using ferric and chromic mixed nitrates were entirely composed of nanocrystalline  $\alpha$ -Fe<sub>2</sub>O<sub>3</sub> phase and a mixture of  $\alpha$  and  $\gamma$ -Fe<sub>2</sub>O<sub>3</sub> phases in case of the solids prepared by mixed sulphates. Various K<sub>2</sub>O and Li<sub>2</sub>O-doped solids consisted of nanocrystalline potassium and lithium ferrites together with ferric oxide phases. However, heavily Li<sub>2</sub>O-doped solids consisted only of LiFe<sub>5</sub>O<sub>8</sub> phase.

- Pure and variously doped solids prepared from mixed sulphates measured specific surface areas bigger than those determined for the other solids. The doping process modified the surface characteristics of the treated adsorbents in a different manner depending on the nature of dopant and its concentration besides the salts used in preparation process.

- Pure mixed solids prepared from ferric and chromic mixed nitrates are more catalytically active than those prepared from mixed sulphates. Doping either with K<sub>2</sub>O or Li<sub>2</sub>O much increased the catalytic activity to an extent proportional to the dopant concentration. However, the increase was pronounced in case of the doped solids prepared from mixed sulphates.

- The doping process did not change the mechanism of the catalytic reaction but increased the concentration of active sites involved in chemisorption and catalysis of CO oxidation reaction without modifying their energetic nature.

#### References

1. Gardener, S.D., Hoflund, G.B., Upchurch, B.T., Schryer, D.R., Kielin, E.J. and Schryer, J., Comparison of the performance characteristics of Pt/SnO<sub>x</sub> and Au/MnO<sub>x</sub> catalysts for low-temperature CO oxidation. *J. Catal.* **129**, 114.
2. Kobayashi, T. Haruta, M. Sano, H. and Nakone, M., *Sens. Actuators Soc. Auto Eng.* **13**, 339 (1988).
3. Kobayashi, T. Haruta, M. and Sano, H., *Chem. Express* **4** (4), 217 (1989).
4. Harrison, P.G. and Willett, M.J., Einstein in Zurich *Nature*, **332**, 337 (1988).
5. Stark, D.S. Crocker, A. and Steward, G.J., A sealed 100-Hz CO<sub>2</sub> TEA laser using high CO<sub>2</sub> concentrations and ambient-temperature catalysts *J. Phys. E. Sci. Instrum.* **16**, 156 (1983).
6. Li, P. Miser, D.E. Rabiei, S. Yadav, R.T. and Hajaligol, M.R. The removal of carbon monoxide by iron oxide nanoparticles. *Appl. Catal. B: Environ.* **43**, 151(2003).
7. Katsuki, H. and Komarneni, S., Role of  $\alpha$ -Fe<sub>2</sub>O<sub>3</sub> Morphology on the Color of Red Pigment for Porcelain. *J. Am. Ceram. Soc.* **86** (1), 183 (2003).
8. Jiang, J.Z., Lin, R., Lin, W., Nielsen, K., Morup, S., Dam-Johansen, K. and Clasen, R., Gas-sensitive properties and structure of nanostructured  $(\alpha - \text{Fe}_2\text{O}_3)_x - (\text{SnO}_2)_1-x$  materials prepared by mechanical alloying. *J. Phys. D: Appl. Phys.* **30**, 1459 (1997).

9. **Huo, L.H., Li, X.L. and Xi, S.Q.**, Gas sensitivity of composite Langmuir–Blodgett films of  $\text{Fe}_2\text{O}_3$  nanoparticle-copper phthalocyanine. *Sensors Actuat. B-Chem.* **71**, 77 (2000).
10. **Li, P., Miser, D.E., Rabiei, S., Yadav, R.T. and Hajaligol, M.R.**, *Appl. Catal. B – Environ.* **1326**, 1(2002) .
11. **Spivey, . J.J.**, 11-Complete catalytic oxidation of volatile organics *Ind. Eng. Chem. Res.* **26**, 2165 (1987).
12. **El-Shobaky, G.A., El-Nabarawy, Th. and Fagal, G.A.**, Surface Properties of Gamma-Irradiated Alumina. *J. Serb. Chem. Soc.* **55**, 21(1990).
13. **El-Shobaky, G.A., Al-Noaimi, A.N., Abdeel-Aal, A. and Ghozza, A.M.**, Catalytic Dehydrogenation and Cracking of Cyclohexane over  $\text{Ni}/\text{Al}_2\text{O}_3$  Solid. *Mater. Lett.* **22**, 167 (1995).
14. **El-Shobaky, G.A., Fagal, G.A., and Mokhtar, M.**, Effect of  $\text{ZnO}$  on Surface and Catalytic Properties of  $\text{CuO}/\text{Al}_2\text{O}_3$  System. *Appl. Catal. A* **155**, 167 (1997).
15. **El-Shobaky, G.A., Fagal, G.A., Ghozza, A.M. and Mokhtar, M.**, Effects of  $\text{Li}_2\text{O}$ -Doping on Surface and Catalytic Properties of  $\text{CuO-ZnO}/\text{Al}_2\text{O}_3$  System. *Colloids and surfaces A* **142**, 17 (1998).
16. **El-Shobaky, G.A., Ghozza, A.M. and El-Shobaky, H.G.**, Effect of  $\text{Li}_2\text{O}$ -Doping on Surface and Catalytic Properties of  $\text{Cr}_2\text{O}_3/\text{Al}_2\text{O}_3$  System. *Adsorp. Sci. Technol.* **16** (6) 415 (1998).
17. **Bolt, P.H., Van Ipenburg, M.E., Geus, J.W. and Habraken, F.H.M.**, *Mat. Res. Symp. Proc.* **344** , 15 (1994).
18. **Ma, Y., Sun, Q., Wu, D., Fan, W.H., Zhang, Y. L. and Deng, J. F.**, Composition effects on the activity of  $\text{Cu-ZnO-Al}_2\text{O}_3$  based catalysts for the water gas shift reaction: A statistical approach. *Appl. Catal. A* **171**, 45 (1998).
19. **El-Shobaky, G.A. EL-Khouly, S.M. Ghozza, A. M. Mohamed**, Surface and Catalytic investigations of  $\text{CuO-Cr}_2\text{O}_3/\text{Al}_2\text{O}_3$  System. *Appl. Catal. A.* **302**, 296 (2006).
20. Quansheng liu, Wenping Ma, Runxia He and Zhanjum Mu, Reaction and characterization studies of an industrial Cr-free iron-based catalyst for high-temperature water gas shift reaction. *Catalyst Today* **106**, 52-56 (2005)
21. **Ghozza, A.M. and El-Shobaky, H.G.** Effect of  $\text{Li}_2\text{O}$ -doping on  $\text{CdFe}_2\text{O}_4$  formation. *Materials Science and Engineering B* **27**, 233–238 (2006)
22. **Lippens, B.C. and DeBoer ; J.H.** Studies on pore systems in catalysts: v.the  $t$  method. *J. Catal.*, **4**, 319 (1965).
23. **El-Shobaky, G.A. El-Nabarawy, Th. and Fagal, G.A.** Surface and Catalytic Properties of  $\text{Li}_2\text{O}$ -Doped  $\text{CuO}/\text{Al}_2\text{O}_3$  Solid. *J. Serb. Chem. Soc.* **55**, 163 (1990).
24. **El-Shobaky, G.A. Fagal, G.A. Ghozza, A.M. and Mokhtar, M.** Effects of  $\text{Li}_2\text{O}$ -Doping on Surface and Catalytic Properties of  $\text{CuO-ZnO}/\text{Al}_2\text{O}_3$  System. *Colloids Surf., A Physicochem. Eng. Asp.* **142**, 17 (1998).

25. El-Shobaky, G.A. Ghozza, A.M. El-Shobaky, H.G. Effect of Li<sub>2</sub>O-Doping on Surface and Catalytic Properties of Cr<sub>2</sub>O<sub>3</sub>/Al<sub>2</sub>O<sub>3</sub> System. *Adsorp. Sci. Technol.* **16**, 415 (1998).
26. El-Shobaky, G.A. Al-Noaimi, A.N. and Dessouki, A.M. Effects of  $\gamma$ -Irradiation and Lithium Doping on the Catalytic Activity of Nickel Aluminium Mixed Oxides. *Surf. Technol.* **26**, 117 (1985).
27. Parravano, G. 27- Catalytic oxidation of CO on NiO catalyst. *Ind. Chem. Eng.* **49**, 266 (1967).
28. Balandin, A.A. *Dokl. Akad. Nauk SSSR* **93**, 55 (1953).

Received 3/ 2/ 2010;  
accepted 23/2/2010)

### الخواص الفيزيوكيميائية والسطحية والحفزية لأكاسيد الحديد والكروم النقيه والمشابهه بأكاسيد البوتاسيوم والليثيوم ومدى تأثيرهم بأملاح الحديد والكروم المستخدمه فى عملية التحضير

جميل على الشوبكى ، عوض ابراهيم أحمد\* و شيماء السيد الشافعى  
قسم الكيمياء الفيزيقيه – المركز القومى للبحوث – الجيزة و قسم الكيمياء – كلية العلوم –  
جامعة المنصورة – المنصورة- مصر .

تم فى هذا البحث تحضير عينات من حفازات مكونه من أكاسيد الحديد والكروم بنسب جزيئيه 0.85 : 0.15: تم تحضيرهم بالتفكك الحرارى لهيدروكسيداتهم عند درجة 500 مؤبوه وتم تحضير مخاليط الهيدروكسيدات بالترسيب المتزامن لمخاليط من نترات وكبريتات الحديد والكروم باستخدام هيدروكسيد الأمونيوم المركز. هذا وقد تم تحضير 6 عينات من الحفازات المشابهه بنسب مختلفه من أكاسيد البوتاسيوم والليثيوم (0.5، 0.75، 1.5 مول %).

أوضحت أهم النتائج أن جميع الحفازات النقيه والمشابهه تتكون من أطوار بللوريه ذات حجم حبيبي متناهى الصغر يتراوح حجمها بين 8-64 نانومتر والحفازات المشابهه تتكون من فيريتات البوتاسيوم والليثيوم بجانب أكاسيد الحديد ( $\alpha$ ،  $\gamma$ ).

المساحه السطحيه النوعيه للحفازات النقيه والمشابهه والمحضرة باستخدام كبريتات الحديد والكروم تتمتع بمساحه سطحيه نوعيه أكبر من الحفازات الأخرى المحضره بنتراتها. تتأثر الخواص السطحيه بالاشابهه بشكل يعتمد على نوع وتركيز ماده المستخدمه فى الاشابهه.

الكفاءه الحفزيه للعينات النقيه المحضره من النترات أكبر من الكفاءه الحفزيه للعينات النقيه المحضره من الكبريتات. تودى عملية الاشابهه بأكاسيد البوتاسيوم والليثيوم الى زياده كبيره فى الكفاءه الحفزيه تتناسب طرديا مع تركيز هذه الأكاسيد مع ملاحظه أن الزيادة فى الكفاءه الحفزيه تكون أكبر بكثير فى حالة الاشابهه بأكاسيد البوتاسيوم للعينات المحضره باستخدام الكبريتات اذا ما قورنت بالعينات المحضره بالنترات. لذا تتمتع العينات المشابهه والمحضره بكبريتات الحديد والكروم بكفاءه حفزيه أكبر من كفاءه الحفازات المشابهه والمحضره من النترات. لا تؤثر عملية الاشابهه فى آلية التفاعل المحفز ولكنها تودى الى زياده فى تركيز المواقع النشطه المشتركه فى التفاعل المحفز.